

GMD 2022 Apr 24 13:53:54

Figure 1: (Left) Larger-scale bird’s eyes perspective of 250 MHz GPR, 50 MHz GPR, static & polarimetric (SPM) and continuous ApRES (cApRES) locations at Ekström Ice Shelf, East Antarctica. (Right) Close-up of the survey grid close to the grounding-zone.

# 1 Summary of ReMeltRadar 2021/22

## 1.1 Objectives

Ocean induced melting at the bottom of Antarctic ice shelves accounts for approximately half of the total ice-mass loss of the Antarctic Ice Sheet. However, processes that govern the heat exchange at the ice-ocean interface are notoriously difficult to observe. Consequently, the coupling between ice- and ocean models rely on a number of poorly constrained parametrizations which require more observational support both spatially and temporally. Moreover, ice-shelves decelerate the ice discharge from tributary glaciers, and the magnitude of deceleration depends on the mechanical rigidity of the ice shelf itself. This rigidity is governed by a non-newtonian, temperature dependent and anisotropic ice-shelf rheology. This also requires observations as model calibration model calibration to todays ice thickness or velocities is strongly underconstrained. ReMeltRadar’s objectives are (1) to quantify the spatial variable ocean-induced melting

from seasonal to centennial timescales, (2) understanding processes that govern ocean-induced melting at sub-kilometers scales, and (3) to map spatial variability in ice anisotropy across different flow regimes. We aim to achieve these objectives with a combination of methods that include model-data fusion (i.e., inversion of the radar stratigraphy using ice-flow forward models), instrument development (i.e., a novel radar combined with an autonomous rover), and profiling with radar polarimetry that is sensitive to the crystal lattice structure.

## 1.2 Field work

The area of interest is the Ekström Ice Shelf, East Antarctica, using the Neumayer station as a logistical hub for field surveys on the ice shelf and in the grounding zone. The first field season took place from 11/2021 – 01/2022. Repeat measurements are planned for the successive field season in 2022/23. Field work was conducted in parts using Skidoos and the Hiluxes operating directly from Neumayer station. In a second phase, data were collected after a 120 km traverse with snow tractors from Neumayer to the southern grounding line of the Ekström Ice Shelf (Fig. 1). Logistics were efficiently shared with the GrouZe Project operating in the same area.

Name	Project	Deployment	Responsibility
Inka Koch (UT)	ReMeltRadar	27.12.21-13.12.22	PulseEkko GPR
Jonathan Hawkins (UCL)	ReMeltRadar	27.12.21-13.12.22	HF ApRES
Reinhard Drews (UT)	ReMeltRadar	27.12.21-13.12.22	Science Coordination
Reza Ershadi (UT)	ReMeltRadar	05.11.21-13.12.22	Rover, SPM
Olaf Eisen (AWI)	ReMeltRadar	05.11.21-13.12.22	Traverse Leader

Table 1: Team composition of ReMeltRadar with members of University of Tübingen (UT), University College London (UCL), and Alfred Wegener Institute (AWI).

### 1.3 Team composition and chronology of data collection

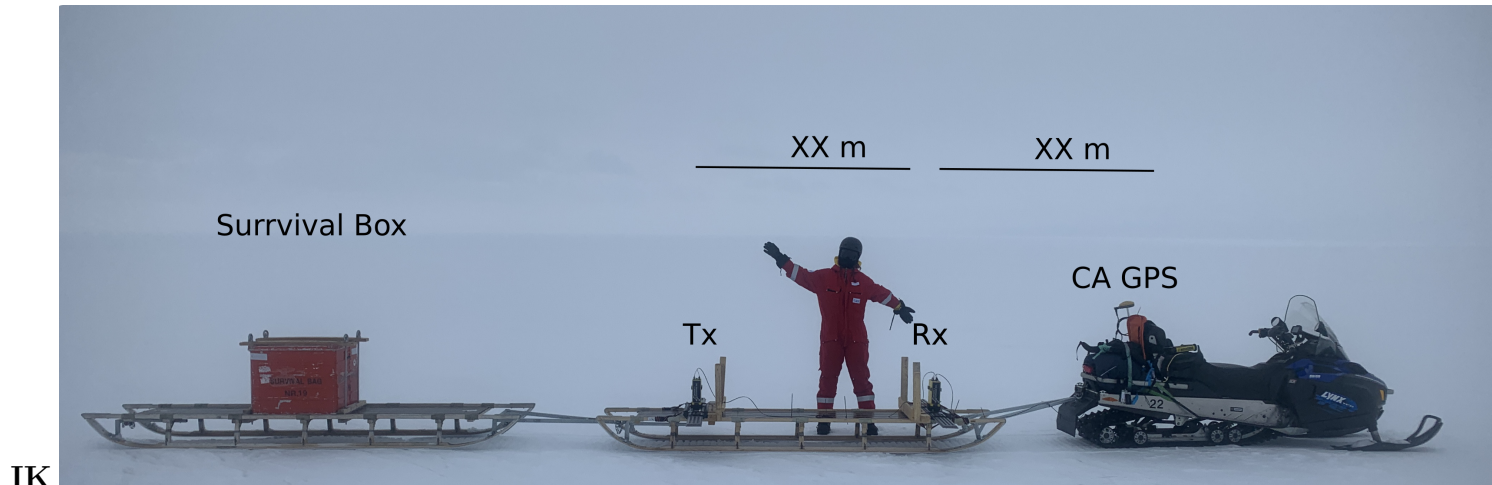
Date	Frequency	Profile	File-ID
28.12.21	50, 100 MHz	Test profiles near NM	<i>PE files</i>
29.12.21	100 MHz	MPA01-MPA03, SPX4-SPX2 near NM	<i>PE files</i>
01.01.22	250 MHz	NM-SPMA25 during traverse	<i>PE files</i>
02.01.22	50 MHz	GZ profiling along flow (SPMA25-SPMA21-GLPE3n-GLPE4s)	<i>PE files</i>
03.01.22	50 MHz	GZ profiling along flow (GLPE4s-GLPE1s-GLPE2n transfer to SPMA25)	<i>PE files</i>
04.01.22	50 MHz	GZ profiling along flow (GLPE7n-GLPE8s-GLPE5s)	<i>PE files</i>
05.01.22	50 MHz	GZ profiling across flow (XX points XX)	<i>PE files</i>
06.01.22	50 MHz	Finegrid along flow (XX points XX)	<i>PE files</i>
09.01.22	50 MHz	Finegrid across flow (XX points XX)	<i>PE files</i>
10.01.22	50 MHz	Along-flow Camp-NM (SPMA21-SPMA10)	<i>PE files</i>
12.01.22	50 MHz	Camp-NM continuation (SPMA10 - XX)	<i>PE files</i>

Table 2: Overview of GPR measurements taken with the PulseEkko radar from Sensors&Software. Details for the system setup and individual profiles are found in Section 3. Operator: I. Koch.  
Here we need a table such as table for each sensor.

## 2 Data structure and initial source codes

RD, JH

### 3 GPR: Data example, field picture, system setup and profile specifics



## 4 SPM: Data example, field picture, system setup and site specifics

This section is written by Reza Ershadi ([Email Me](#))

The SPM points were measured in two different ways.

- We drove to the point by Hilux. We set up the system (ApRES and antenna) every time at each point. In this method, the antennas were directly on the snow surface (fig. 2). The coordinates and date of the measurements are written in table (3).
- We fixed the system (ApRES and antenna) inside the sleds and drove to the points by a snowmachine (fig. 5). The coordinates and date of the measurements are written in table (4).

More information on these points is in the following path:

..\\Tex\\Info\\RE\_SPM\_Points\_Info.csv

..\\Tex\\Info\\RE\_BulletPointReport.txt

#### 4.1 SPM: Antenna directly on snow surface

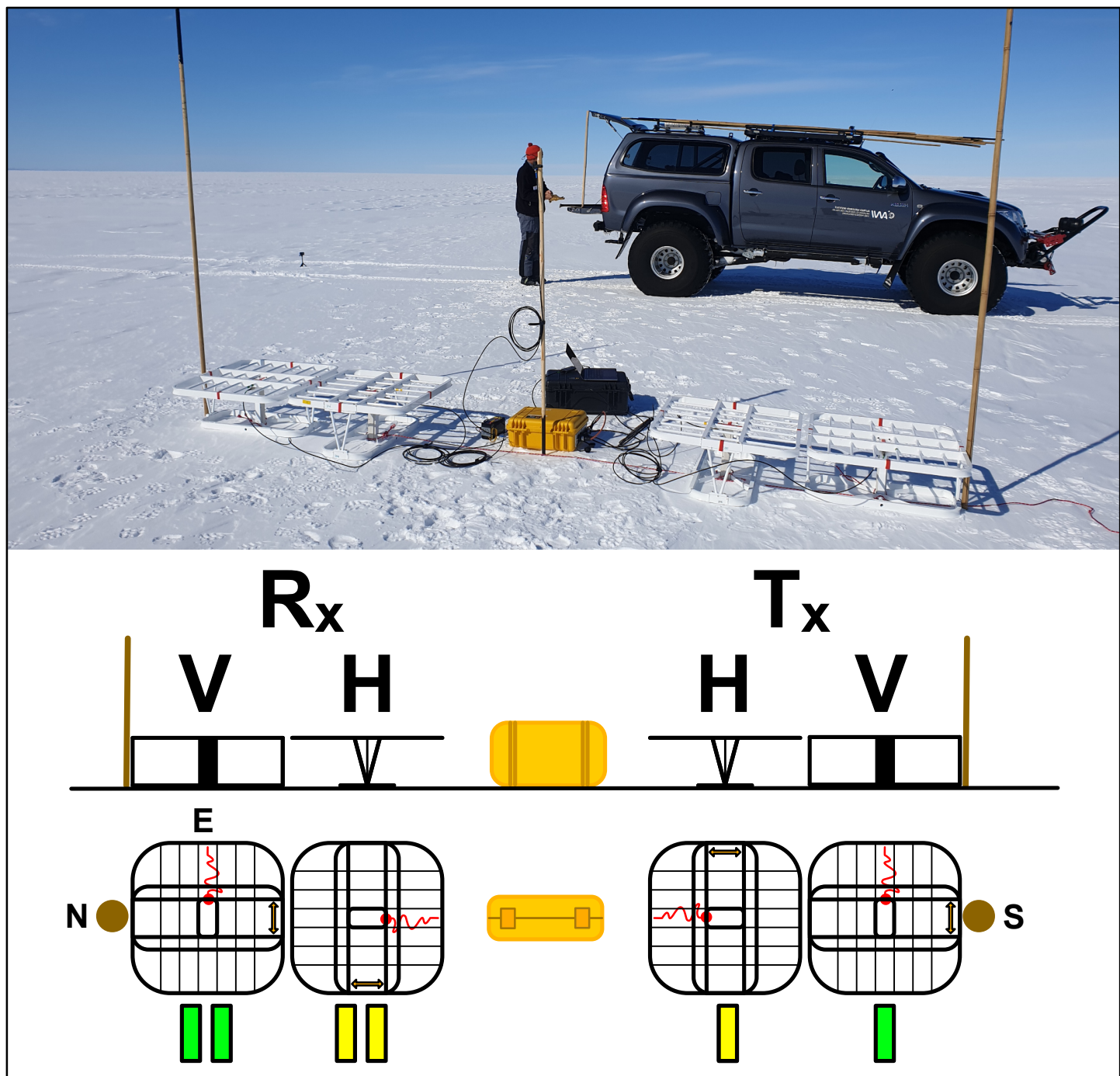


Figure 2: SPM four antenna (mimo) measurements. Antenna directly on the snow surface. The yellow and green rectangles are the tape sign on each antenna. The brown sticks and circles are the bamboo poles. The system was positioned in a way that T was always in the South direction.

Name	Date	Latitude	Longitude	pRES	Note
SPM X 04	06.12.2021			127	Unattened mimo test with RTK GPS running
SPM A 01	06.12.2021			127	Note
SPM A 04	06.12.2021			127	Note
SPM A 06	07.12.2021	S70 54.6083	W8 35.0011	127	Note
SPM A 08	07.12.2021	S70 59.6685	W8 29.5190	127	Note
SPM A 10	07.12.2021	S71 04.8188	W8 24.1606	127	Note
SPM A 12	07.12.2021	S71 09.9336	W8 19.5682	127	Note
SPM A 11	07.12.2021	S71 07.3516	W8 21.8561	127	Note
SPM A 09	07.12.2021	S71 02.2326	W8 26.9498	127	Note
SPM A 07	07.12.2021	S70 57.1200	W8 32.0608	127	Note
SPM A 05	07.12.2021	S70 52.1103	W8 38.0142	127	Note
SPM X 12	07.12.2021	S70 48.5407	W8 37.3807	127	Note
SPM X 05	08.12.2021	S70 42.1876	W8 36.2362	127	Note
SPM X 06	08.12.2021	S70 42.9845	W8 42.2801	127	Note
SPM A 02	08.12.2021	S70 44.6456	W8 47.2300	127	Note
SPM A 03	08.12.2021	S70 47.0996	W8 43.9270	127	Note
SPM X2 13	08.12.2021	S70 49.5042	W8 44.3598	127	Note
SPM X2 12	08.12.2021	S70 48.6233	W8 38.4010	127	Note
SPM X3 01	01.01.2022	S71 0.1622	W7 37.8862	127	Note
SPM X3 02	01.01.2022	S71 0.8448	W7 44.6390	127	Note
SPM X3 03	01.01.2022	S71 1.0425	W7 46.5675	127	Note
SPM X3 04	01.01.2022	S71 1.4077	W7 50.0373	127	Note
SPM X3 05	01.01.2022	S71 1.5366	W7 52.3067	127	Note
SPM X3 06	01.01.2022	S71 1.6515	W7 52.5199	127	Note
SPM X3 07	01.01.2022	S71 2.0236	W7 56.2648	127	Note
SPM X3 08	01.01.2022	S71 2.4512	W8 0.4169	127	Note
SPM X3 09	01.01.2022	S71 8.2488	W8 8.3205	127	Note
SPM X3 10	01.01.2022	S71 4.0086	W8 16.2397	127	Note
SPM A 13	01.01.2022	S71 12.5541	W8 17.6910	127	Note
SPM A 14	01.01.2022	S71 15.2070	W8 16.5035	127	Note
SPM A 15	01.01.2022	S71 17.8907	W8 16.5801	127	Note
SPM A 16	01.01.2022	S71 20.5795	W8 16.6960	127	Note
SPM A 17	01.01.2022	S71 23.2723	W8 16.9177	127	Note
SPM A 18	01.01.2022	S71 25.9609	W8 17.1657	127	Note
SPM A 25	04.01.2022	S71 43.5428	W8 35.8674	128	Note

Table 3: SPM on surface info

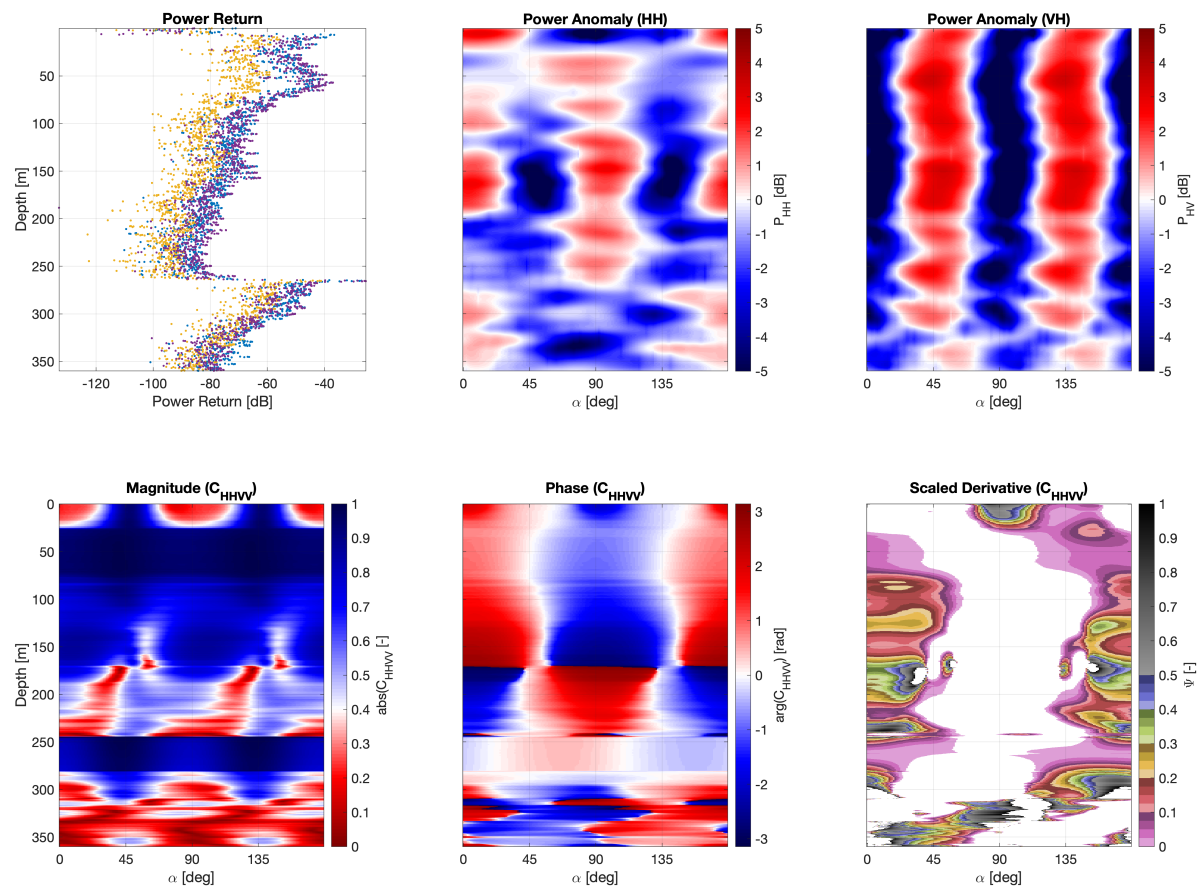


Figure 3: Data example from SPM\_X\_05 (floating ice - far from the GZ)

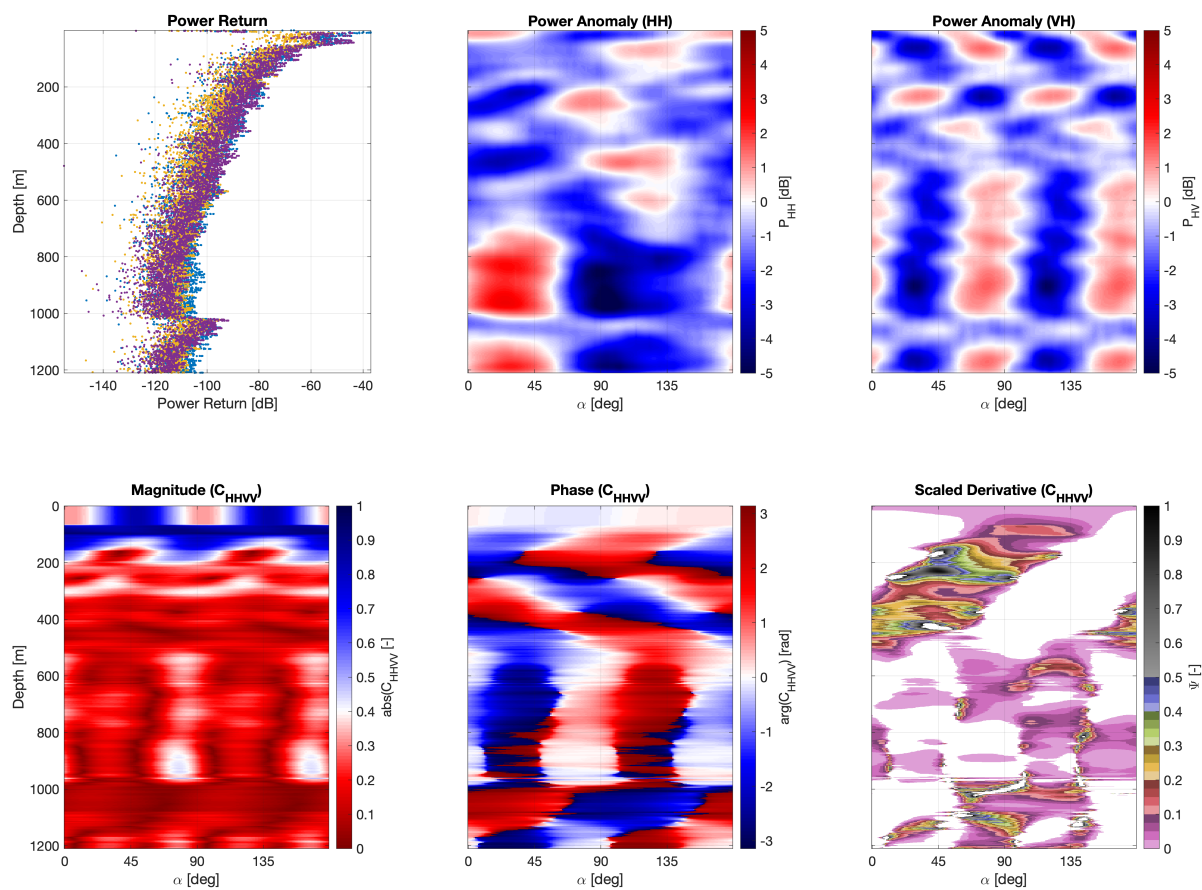


Figure 4: Data example from SPM\_A\_25 (grounded ice - very close to the GZ)

## 4.2 SPM: Antenna inside the sleds

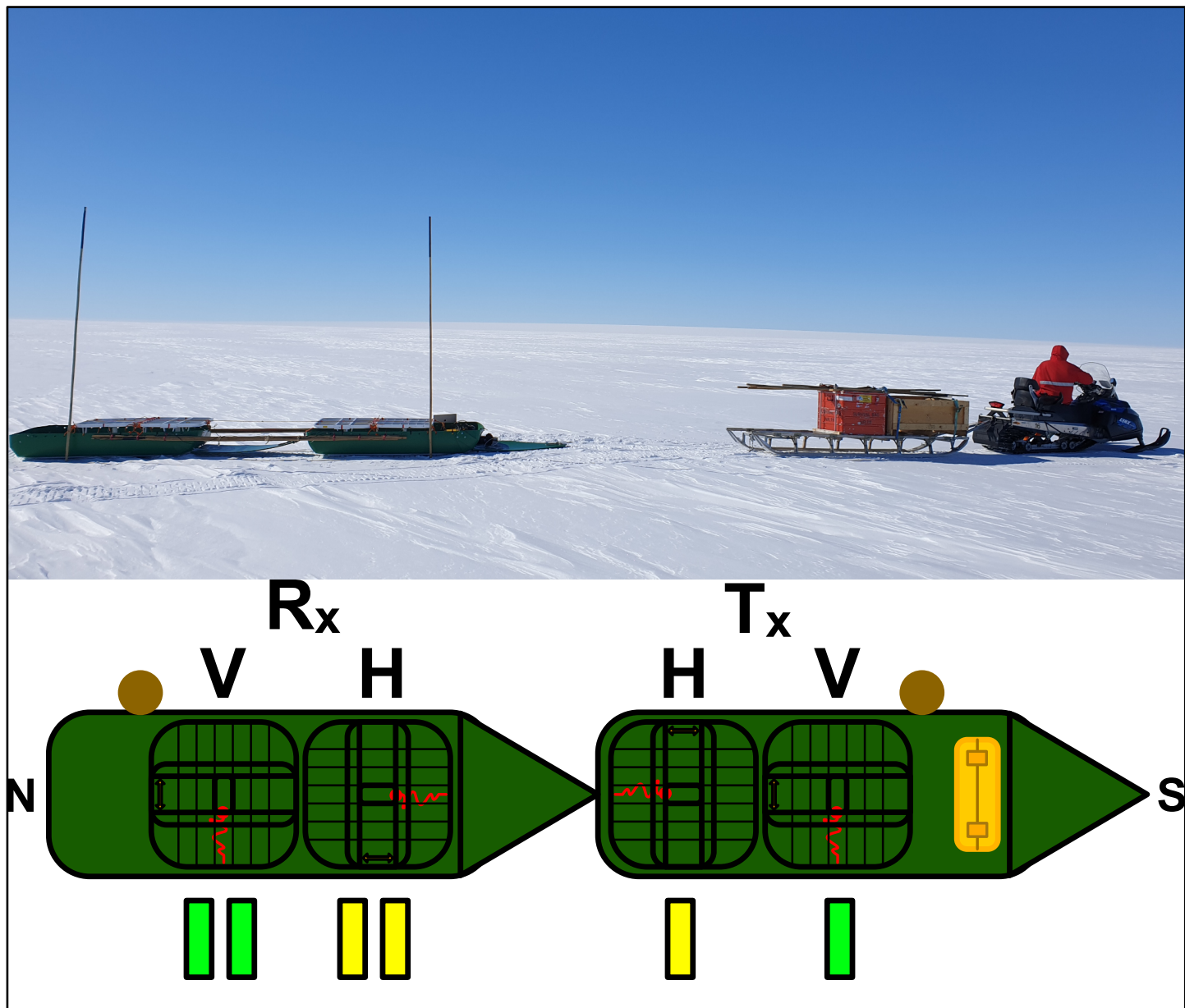


Figure 5: SPM four antenna (mimo) measurements. Antenna inside sleds. The yellow and green rectangles are the tape sign an each antenna. The brown sticks and circles are the bamboo poles. The system was positioned in a way that T was always in the South direction.

Name	Date	Latitude	Longitude	pRES	Note
SPM X 01	10.12.2021	S70 38.9781	W8 12.1931	127	
SPM X2 11	11.12.2021	S70 47.7299	W8 32.4452	127	
SPM X2 10	11.12.2021	S70 46.8444	W8 26.5088	127	
SPM X2 09	11.12.2021	S70 45.9602	W8 20.4776	127	
SPM X 03	12.12.2021	S70 40.5602	W8 24.2193	127	
SPM X 02	12.12.2021	S70 39.7987	W8 17.4478	127	
SPM X2 01	13.12.2021	S70 43.2433	W8 2.8528	?	
SPM X2 02	13.12.2021	S70 43.5002	W8 4.3377	?	
SPM X2 03	13.12.2021	?	?	?	double check needed
SPM X2 04	13.12.2021	?	?	?	double check needed
SPM X2 05	13.12.2021	S70 44.145	W8 8.7386	?	
SPM X2 06	13.12.2021	S70 44.4317	W8 10.4649	?	
SPM X2 07	13.12.2021	S70 44.7319	W8 12.5599	?	
SPM X2 08	13.12.2021	S70 45.0474	W8 14.6026	?	
SPM A 22	7.01.2022	S71 36.3400	W8 24.1557	127	Same setup as rover in traverse
SPM A 19	7.01.2022	S71 28.6556	W8 17.4667	127	Same setup as rover in traverse
SPM A 20	7.01.2022	S71 31.3291	W8 18.3103	127	Same setup as rover in traverse
SPM A 21	7.01.2022	S71 33.8910	W8 20.5898	127	Same setup as rover in traverse
SPM A 23	7.01.2022	S71 38.7621	W8 27.8876	127	Same setup as rover in traverse
SPM A 24	7.01.2022	S71 41.1405	W8 31.9045	127	Same setup as rover in traverse
SPM X4 01	08.01.2022	S71 25.0643	W8 45.4317	127	Same setup as rover in traverse
SPM X4 02	08.01.2022	S71 54.3048	W8 43.9249	127	Same setup as rover in traverse
SPM X4 03	08.01.2022	S71 45.5403	W8 42.3649	127	Same setup as rover in traverse
SPM X4 04	08.01.2022	S71 45.7764	W8 40.8149	127	Same setup as rover in traverse
SPM X4 05	08.01.2022	S71 46.0135	W8 39.2839	127	Same setup as rover in traverse
SPM X4 06	08.01.2022	S71 46.2455	W8 37.7977	127	Same setup as rover in traverse
SPM X4 07	08.01.2022	S71 46.4827	W8 36.1669	127	Same setup as rover in traverse
SPM X4 08	08.01.2022	S71 46.7199	W8 34.6045	127	Same setup as rover in traverse

Table 4: SPM on sled info

## 5 MP\_A (profiling)

This section is written by Reza Ershadi ([Email Me](#))

The purpose here was to measure a 1000 m profile with 1.5 m spacing with all the antennas positioned in the H direction. The system was directly connected to an RTK GPS for precise positioning. We had many problems with this profile, including the RTK signal, constant ApRES disconnection and typical rover problems. Therefore, we could not finish the 1000 m profile with 1.5 m spacing. The position of the profile and measured points are stored in our log files.

Add detailed information about the 3 metal pieces. (?)

The MP\_A profile has been done with two different methods.

- We pulled the whole sled system manually for 100 m with 1.5 m spacing (fig. 6).
- We connected the sled system to the rover for a 1000 m profiling with 1.5 m spacing (fig. 7)

### 5.1 Manually pulling the sleds

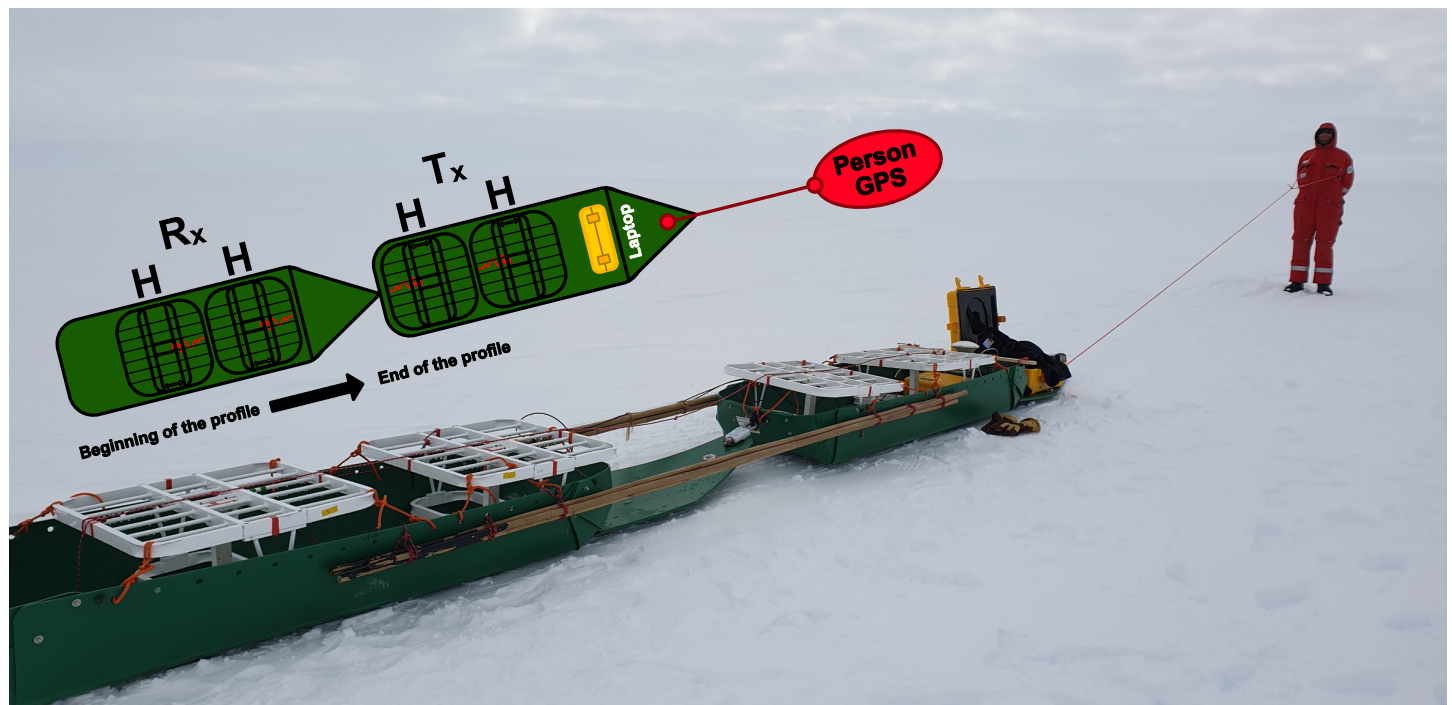


Figure 6: Manually pulling the ApRES and sleds

## 5.2 Using the rover



Figure 7: Pulling the ApRES and sleds using the rover

## 6 HF ApRES

### 6.1 System Overview

The HF ApRES is a frequency modulated continuous wave (FMCW) radar with a bandwidth of 20 MHz to 40 MHz. It builds upon the existing phase-coherent radar architecture of the ApRES<sup>1</sup> but uses a modified radio front-end to operate at the reduced bandwidth described. In addition to the radar, the HF ApRES makes use of two 'wire-mesh dipole' antennas - one each for the transmitter and receiver, and a 12V 7 A h lead-acid battery for power. Both the HF ApRES radar unit and the 'wire-mesh dipole' antennas had not been previously deployed on a polar ice shelf. The objectives for the HF ApRES system were therefore to test and validate its performance, then conduct a synthetic aperture radar survey of the ice-ocean interface of the ice shelf.

#### 6.1.1 System Equipment Listing

- 1x HF ApRES (VAB Issue C and RMB2F in Pelicase)
- 2x Wire-Mesh Dipole Antennas
- Clusons 12V 7 A h Lead Acid Battery
- 4x Radiall RG213 5 m 50Ω RF Cables (R284C0351044)
- 2x Gigatronix LBC400 25 m 50Ω RF Cables (APX2KDP6ZAB40L)
- 2x 10 dB RF attenuators
- Various RF connectors
- Trimble R9s Modular GNSS System (receiver and base station with UHF radio link)
- Bamboo and 10mm kernmantle rope for towed configuration.

### 6.2 Testing Summary

Testing was first conducted with the wire-mesh antennas to verify that they met the power transfer characteristics predicted through simulation. Once verified, a setup with the full HF ApRES system was configured and issues were found with strong coupling between the transmit and receive antennas. After further testing, it was found that broadside orientation of the antennas and increased separation reduced the direct coupling between the antennas sufficiently for clean deramped signals to be recorded.

---

<sup>1</sup>P. Brennan, L. Lok, K. Nicholls and H. Corr, "Phase-sensitive FMCW radar system for high-precision Antarctic ice shelf profile monitoring", IET Radar, Sonar & Navigation, vol. 8, no. 7, pp. 776-786, 2014. Available: 10.1049/iet-rsn.2013.0053.

Date	Frequency	Profile	File-ID
27.12.21	30 MHz	Testing of antennas and HF ApRES near Neumayer	<i>Testing.db</i>
28.12.21	30 MHz	(as above)	<i>Testing.db</i>
29.12.21	30 MHz	(as above)	<i>Testing.db</i>
30.12.21	30 MHz	(as above)	<i>Testing.db</i>
02.01.22	30 MHz	Testing of HF ApRES at Camp	<i>Testing.db</i>
03.01.22	30 MHz	(as above)	<i>Testing.db</i>
04.01.22	30 MHz	(as above)	<i>Testing.db</i>
05.01.22	30 MHz	(as above)	<i>Testing.db</i>
06.01.22	30 MHz	Testing of HF ApRES at Camp and relocate to GL	<i>Testing.db</i>
07.01.22	30 MHz	Initial measurements of start-stop survey at GL	<i>Testing.db,</i> <i>StartStop.db</i>
08.01.22	30 MHz	Complete measurement of start-stop survey at GL and attempt kinematic surveys	<i>Testing.db,</i> <i>StartStop.db</i>

Table 5: Overview of measurements taken with HF ApRES System. Individual data files are described within the *Testing* and *StartStop* databases. Schema for the databases can be found in the Appendix A of this report.

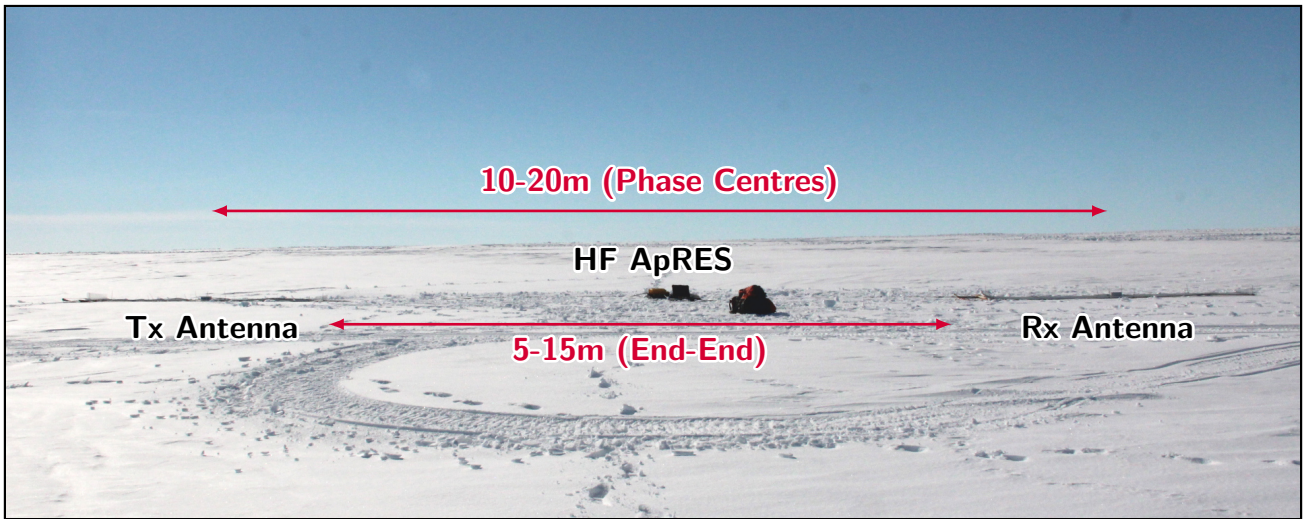


Figure 8: Deployed HF ApRES radar positioned in centre of transmit (Tx) and receive (Rx) antennas in endfire configuration.

### Wire-Mesh Dipole Antennas

The wire-mesh dipole antennas were each tested with an SDRKits Vector Network Analyzer (VNA) which allows for the measurement of the antenna reflection coefficient ( $\Gamma$ ). The reflection coefficient is calculated from the scattering parameters (s-parameters) measured by the VNA, where  $S_{11}$  refers to the complex phasor ratio between the scattered and incident voltages from the antenna. The reflection coefficient can therefore be used to infer the ratio of incident power to the antenna which is 'accepted' and sets an upper bound on the radiation efficiency. The radiation efficiency of the antenna is the ratio of incident power to the antenna that is actually radiated rather than scattered back to the radar, or lost through conduction within the antenna structure. Radiation efficiency is difficult to measure in a field environment, hence the reflection coefficient is used to determine an upper bound.

$$|\Gamma|_{\text{dB}} = 20 \log_{10} |S_{11}| \quad (1)$$

The measured reflection coefficient of the wire-mesh dipole antennas from tests on 28<sup>th</sup> December is shown in Figure 9. Within the field of antenna engineering, a reflection coefficient of less than  $-10 \text{ dB}$  across the desired signal bandwidth, i.e. greater than 90% of power accepted by the antenna, is deemed to be acceptable. It can be seen that during initial tests conducted 500 m south-west of Neumayer Station the antennas have a measured  $|S_{11}|_{\text{dB}}$  of less than  $-10 \text{ dB}$  across the desired signal bandwidth of 20 MHz to 40 MHz. Discussion regarding the antenna orientation can be below.

**Note:** After transport of the antennas from Neumayer III to the grounding line camp, it was found that one of the centre-pin conductors on the antenna arms had become loose, likely due to a dry solder joint.

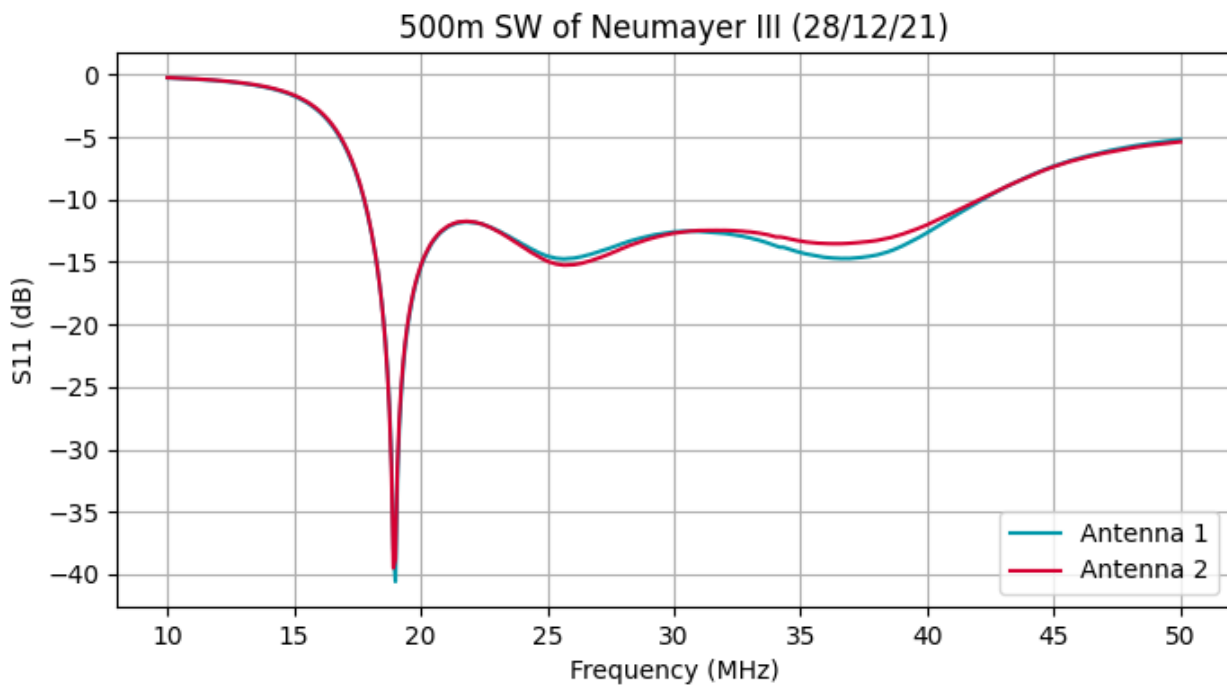


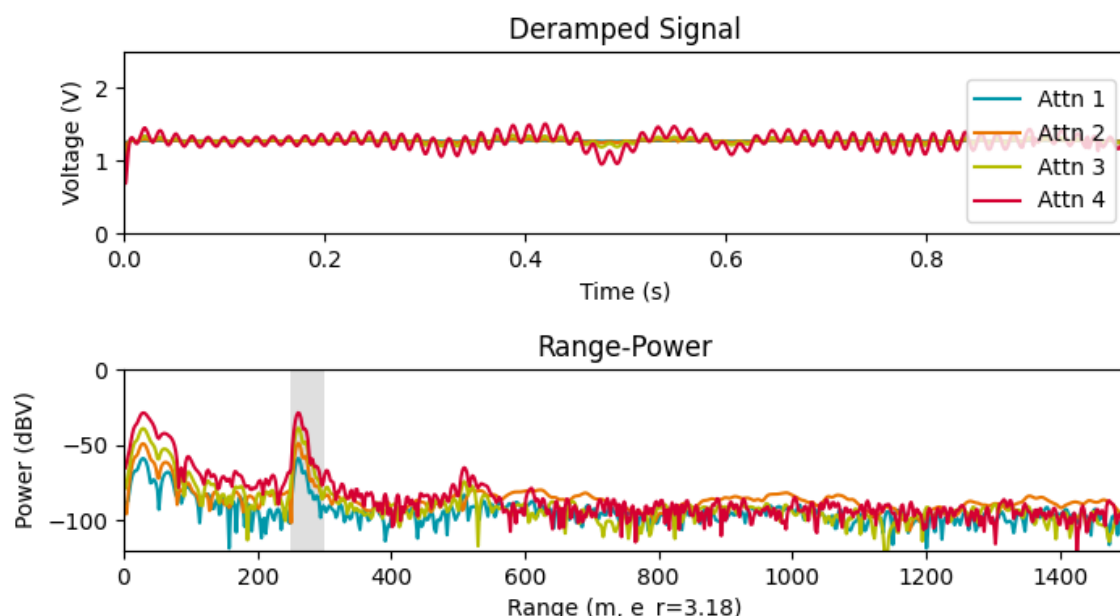
Figure 9: Measured power reflection coefficient for HF wire-mesh dipole antennas, positioned approximately 500 m south-west of Neumayer Station.

## HF ApRES Radar

Figure 6 shows a measured test profile at Neumayer Station where it was discovered that the receiving antenna of the HF ApRES radar was disconnected. A radar echo from is visible at approximately 250 m depth, which corresponds with the expected thickness of the ice shelf in the vicinity of the station. The working explanation for the clear, high signal-to-noise ratio (SNR) echo from the ice-shelf base with no receiving antenna is that the echo is received by the transmitting antenna and coupled via the 5V power rail to the receive RF path. Other coupling paths, such as from the transmit antenna to the mixer input or via a reflection from the disconnected receiver port, are ruled out because they would not exhibit the 10 dB step change in power with the value of the receive attenuator. An alternative explanation to be explored through simulation is that the received signal is coupled through the coaxial cable connected to the receive port, acting as a poorly matched whip antenna.

Reconnecting the receiver antenna, as shown in Figure 7 results in significant distortion visible in the time-domain FMCW voltage signal, matched with the reduced SNR seen in the range-power profile. Overall power is increased relative to Figure 6, which gives confidence that the antenna was not connected and has been successfully reconnected in the second dataset. The distortion is characteristic of 'clipping' where the recorded signal exceeds the voltage range of the analogue-to-digital converter and the output is subsequently 'clipped' to be within this range. The evidence of clipping, at low frequencies corresponding

Table 6: Antennas aligned E-W, no receive antenna connected but clear return from ice-shelf base and double bounce.



**Filename** 2021-12-28-213752.dat

Param.	Value	Param.	Value
<b>AF Gain</b>	6,6,6,6	<b>RF Attn.</b>	30,20,10,0
<b>Subbursts</b>	10	<b>Period (<math>T</math>)</b>	1.000 s
<b>Bandwidth</b>	20 - 40 MHz	<b>Power Code</b>	127
<b>Batt. Volt.</b>	12.129 V	-	-

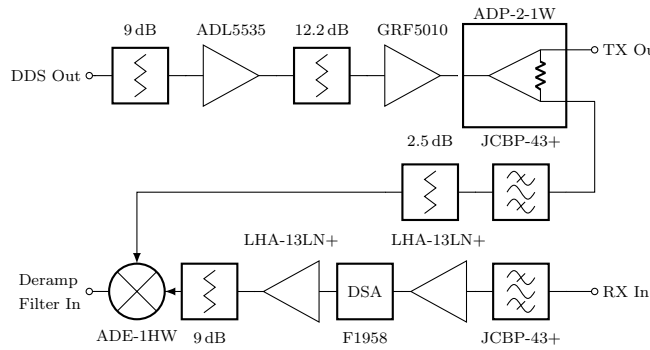
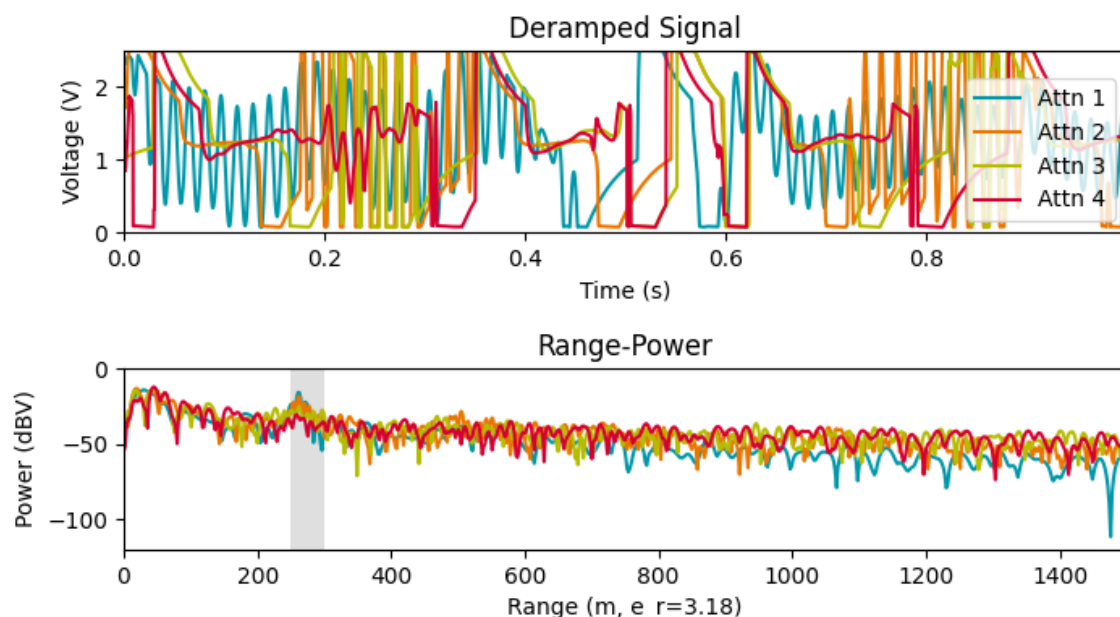


Figure 10: System level diagram of the RMB2F radar, showing the signal path from the direct digital synthesiser (DDS) to the transmit output, receiver input and ouput deramped FMCW signal.

to short range echoes suggests that the direct coupling between the transmit and receive antennas is higher than experienced from a previous deployment of the HF ApRES radar on an Alpine glacier.

**Antenna orientation** was shown to influence coupling between the transmit and receive antennas and the presence of high-power low frequency signals in the deramped FMCW voltage signal. Broadside refers to the antennas positioned such that their phase centres are in line with the survey direction and their longest axes are orthogonal to the survey direction. Endfire refers to the antennas positioned such that their longest axes are parallel to the survey direction. Experiemnts repeated at Neumayer Station (Figures 8 and 9) and the grounding line camp (Figures 10 and 11) show that thwne antennas are aligned in a 'broadside' configuration they exhibit reduced near-range coupling compared to antennas separated by the same distance in an 'endfire' configuration. The HF ApRES was then reconfigured to be operated with the SubZero rover in a broadside configuration, with an increased separation between the transmit and receive antennas of 40 m.

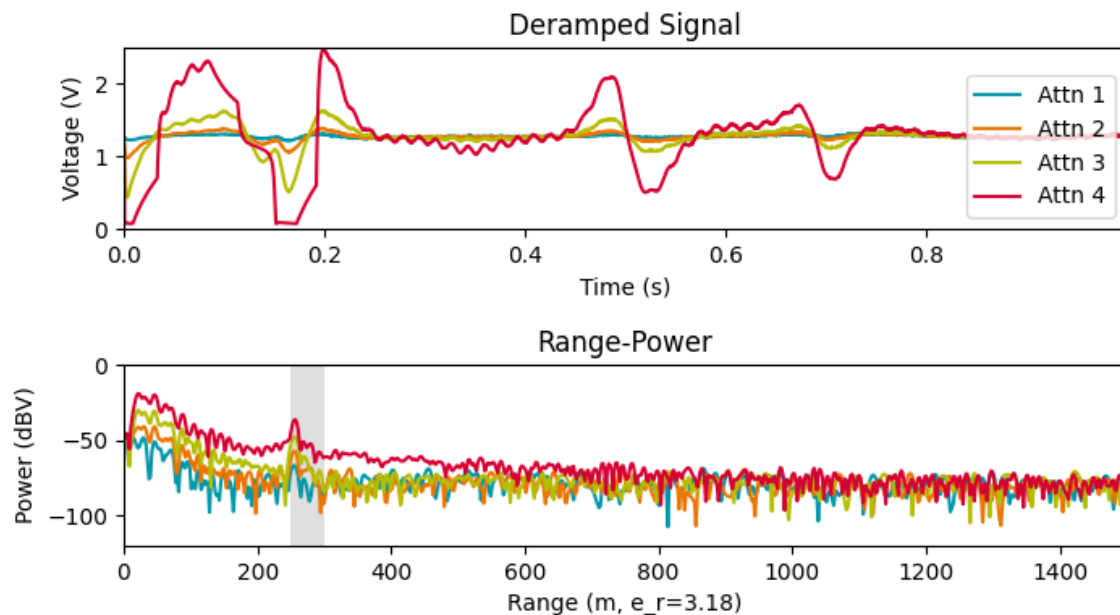
Table 7: Antennas aligned E-W, receive antenna reconnected and low-frequency (i.e. near range) distortion present in signal resulting in reduced signal-to-noise ratio.



**Filename** 2021-12-28-214326.dat

Param.	Value	Param.	Value
<b>AF Gain</b>	6,6,6,6	<b>RF Attn.</b>	30,20,10,0
<b>Subbursts</b>	10	<b>Period (<math>T</math>)</b>	1.000 s
<b>Bandwidth</b>	20 - 40 MHz	<b>Power Code</b>	127
<b>Batt. Volt.</b>	12.158 V	-	-

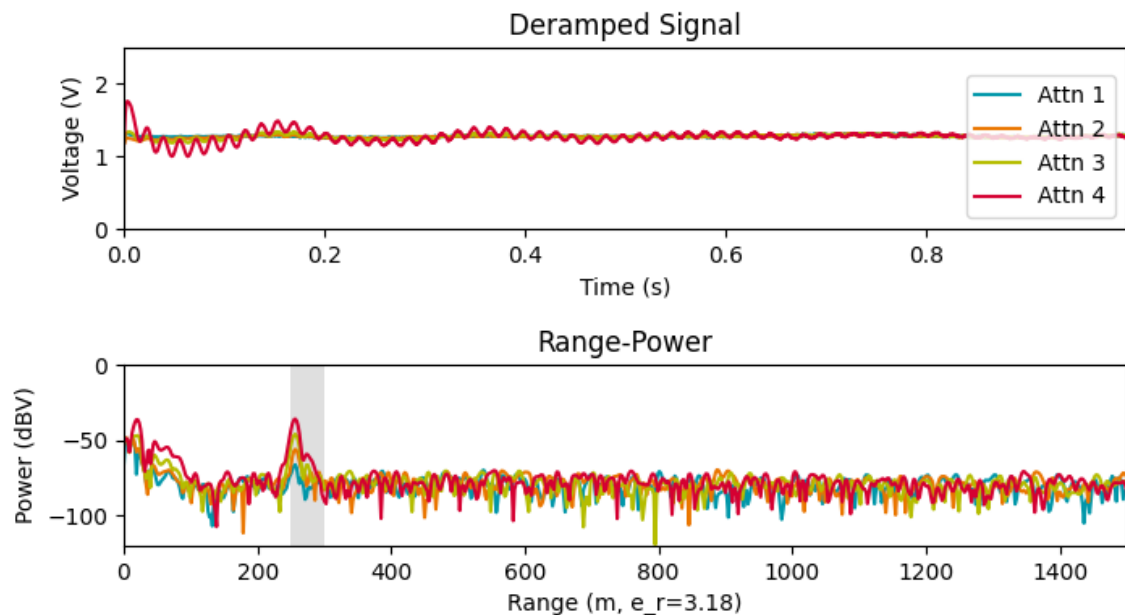
Table 8: **Antenna Orientation: Endfire, Neumayer.** No additional attenuations. Antennas rotated so they are aligned N-S and cables N-S. Similar to above but with noise in upper layers. 14m separation. Cables 'smooth' in line with antennas. Reduced power code to 0.



**Filename** 2021-12-29-215659.dat

Param.	Value	Param.	Value
AF Gain	6,6,6,6	RF Attn.	30,20,10,0
Subbursts	1	Period ( $T$ )	1.000 s
Bandwidth	20 - 40 MHz	Power Code	0
Batt. Volt.	12.266 V	-	-

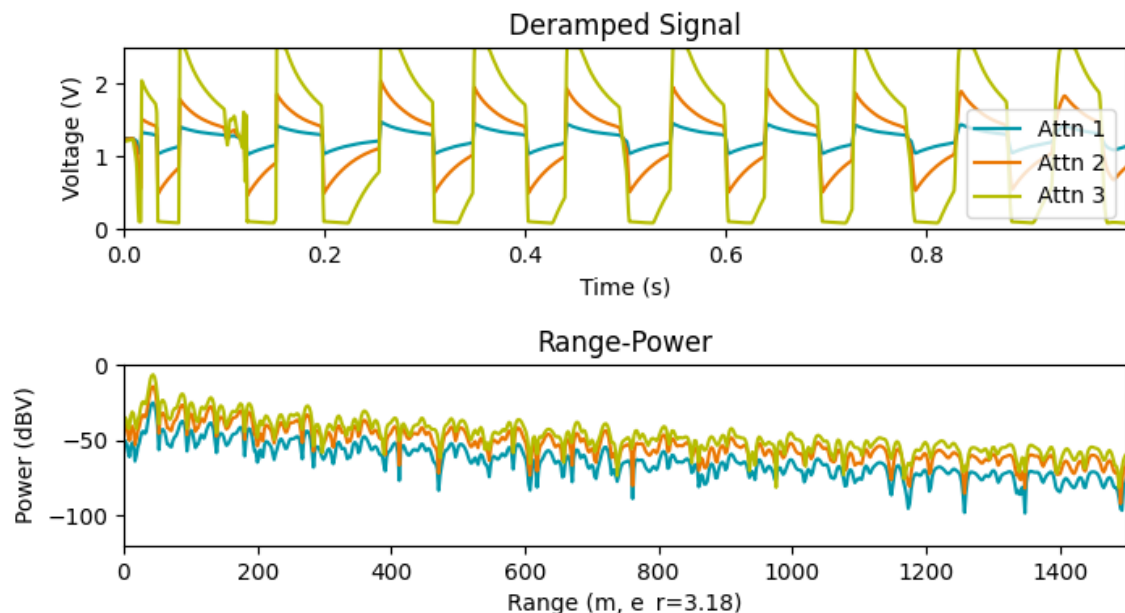
Table 9: **Antenna Orientation: Broadside, Neumayer.** No additional attenuations. Antennas rotated so they are aligned E-W but Tx at N and Rx at S. Similar to above but with noise in upper layers. 14m separation. Cables 'smooth' in line with antennas. Reduced power code to 0.



**Filename** 2021-12-29-220442.dat

Param.	Value	Param.	Value
AF Gain	6,6,6,6	RF Attn.	30,20,10,0
Subbursts	1	Period ( $T$ )	1.000 s
Bandwidth	20 - 40 MHz	Power Code	0
Batt. Volt.	12.258 V	-	-

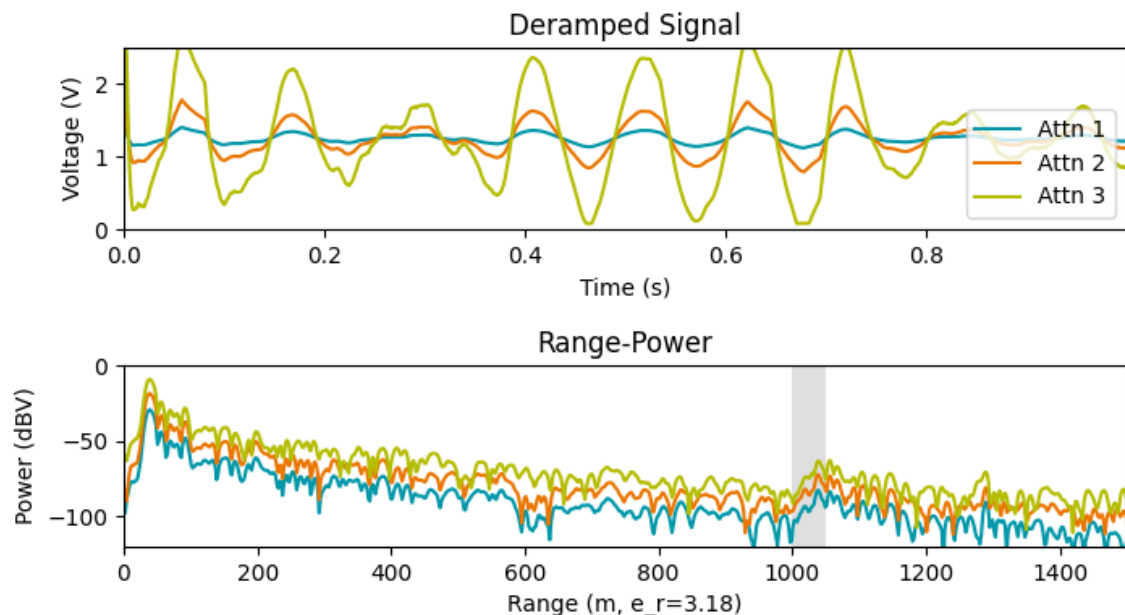
Table 10: **Antenna Orientation: Endfire, Grounding Line.** Additional attenuator 10dB Rx, 0dB Tx. Cable length Tx 25m, Rx 25m and separate antennas to maximum length (30m). Antennas return to endfire. Clipping across all AF settings. No clear basal return.



**Filename** 2022-01-05-174254.dat

Param.	Value	Param.	Value
<b>AF Gain</b>	-14,-4,6	<b>RF Attn.</b>	0,0,0
<b>Subbursts</b>	40	<b>Period (T)</b>	1.000 s
<b>Bandwidth</b>	20 - 40 MHz	<b>Power Code</b>	127
<b>Batt. Volt.</b>	12.238 V	-	-

Table 11: **Antenna Orientation: Broadside, Grounding Line.** Additional attenuator 10dB Rx, 0dB Tx. Increase Tx cable to 25m (Rx 5m) and separate antennas to maximum length (30m). Antennas rotated broadside. Bed clearer (higher SNR)? Some clipping in signal. Repeated as before - ringing reduced?



**Filename** 2022-01-05-171029.dat

Param.	Value	Param.	Value
<b>AF Gain</b>	-14,-4,6	<b>RF Attn.</b>	0,0,0
<b>Subbursts</b>	40	<b>Period (T)</b>	1.000 s
<b>Bandwidth</b>	20 - 40 MHz	<b>Power Code</b>	127
<b>Batt. Volt.</b>	12.238 V	-	-

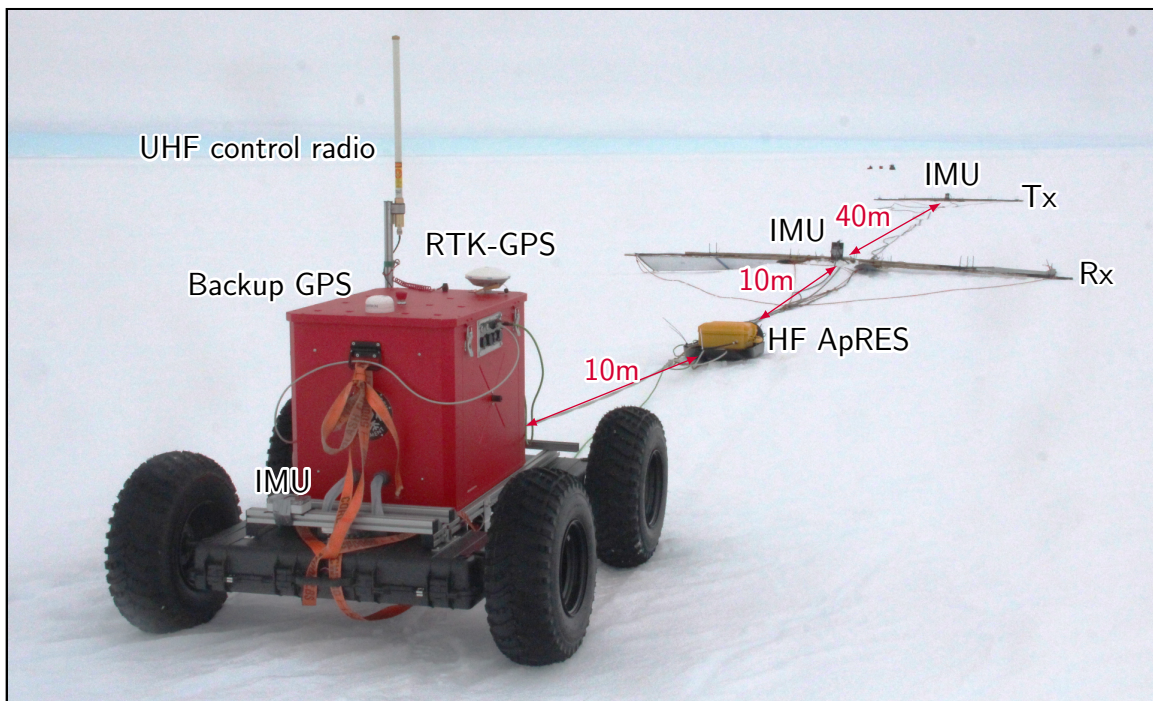


Figure 11: SubZero rover and HF ApRES configuration used for start-stop and kinematic synthetic aperture radar acquisitions at groundling line.

### 6.3 Synthetic Aperture Radar Measurements

The test site chosen for the HF ApRES SAR measurements was selected to coincide with the series of basal terraces observed in the PulseEKKO data located in the finely gridded region of Figure 1. The HF ApRES system was towed into position on 7<sup>th</sup> January, configured according to 11 and initial testing was conducted, including the resolution of a software navigation issue with the rover. Two modes of measurement were conducted with the HF ApRES: a start-stop profile where the instrument was repositioned in steps of 1 m increments along the desired profile direct, and kinematic profiles where the radar was set to continuously measure while towed along the profile by the SubZero rover at speeds of approximately  $0.7 \text{ m s}^{-1}$  to  $1 \text{ m s}^{-1}$ . For all measurement modes, the radar was configured with the parameters listed in Table 12. The VV notation for the polarisation is consistent with that of the rover-towed VHF system, however the precise polarisation response of the wire-mesh dipole antennas has not been measured.

Parameter	Symbol	Value	
Centre Frequency	$f_c$	30	MHz
Bandwidth	$B$	20	MHz
Pulse Duration	$T$	1	s
Transmit Power	$P_T$	0.1	W
AF Gain	$G_{AF}$	6	dB
RF Attenuation	$A_{RF}$	10	dB
RF Atten. (External)	$A_{RFExt}$	10	dB
Antenna Separation	$S_{Ant}$	40	m
Rover Separation	$S_{Rov}$	10	m
Polarisation	-	VV	-

Table 12: Radar configuration parameters common to both the start-stop and kinematic the HF ApRES SAR measurements

#### 6.3.1 Start-Stop Measurement

On the 7<sup>th</sup> January, 192 m of the intended profile was covered . The rover was left in position overnight and the profile was resumed to cover the remaining 710 m over approximately 5 hours, including approximately

one hour of cumulative downtime. The Trimble R9s base station was set up approximately 40 m away from the profile at its centre. The RINEX files generated by the GNSS receivers at the base station and on the rover were processed using the Canadian Spatial Reference System Precise Point Positioning service<sup>2</sup> and are shown in Figure 14. There are tidal and ice flow components present in the raw position data. The ice velocity ( $v$ ) is assumed constant along the length of the profile from analysis of the 120 m composite ITS\_LIVE data for 2020. The tidal components of the measured elevation were analysed using the Tidal Fitting Toolbox <sup>3</sup> but have not yet been validated with external data. It is assumed that the tidal components are also locally invariant and therefore the relative position of the rover to the base is initially found through subtraction of the base station coordinates from the rover coordinates. Phase and power of raw data is shown in Figure 12.

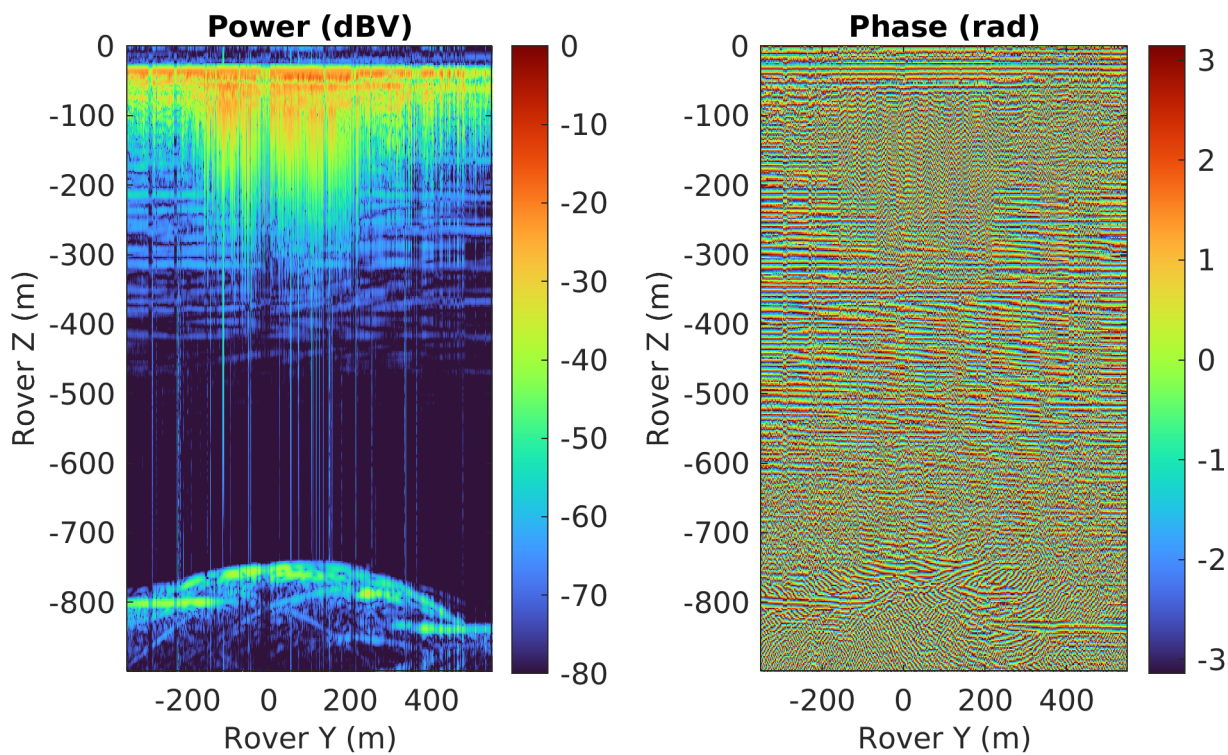


Figure 12: Phase and power of raw, unprocessed ApRES data collected along the profile.

Initial SAR processing of the dataset was performed using an interpolated sinc routine using the MATLAB<sup>®</sup> ApRESProcessor library<sup>4</sup> with a constant velocity travel-time model using a dielectric permittivity for ice of 3.15. Antenna positions were modelled to be 50 m and 10 m behind the rover, in the direction of the image plane, as per the system setup indicated in Figure 11. For the intial pass, bursts with low signal to noise ratios compared to the mean of the dataset were excluded however further passes

<sup>2</sup>Full details can be found in `Raw/RTKGPS/ApRES/Rover/HF/processing_notes.md`

<sup>3</sup><https://uk.mathworks.com/matlabcentral/fileexchange/19099-tidal-fitting-toolbox>

<sup>4</sup><https://github.com/jonodhawkins/apresprocessor>

will select individual chirps from these bursts to maximise the number of radar locations at which the backprojection is performed. Results of the backprojection in power and phase are shown in Figure 13.

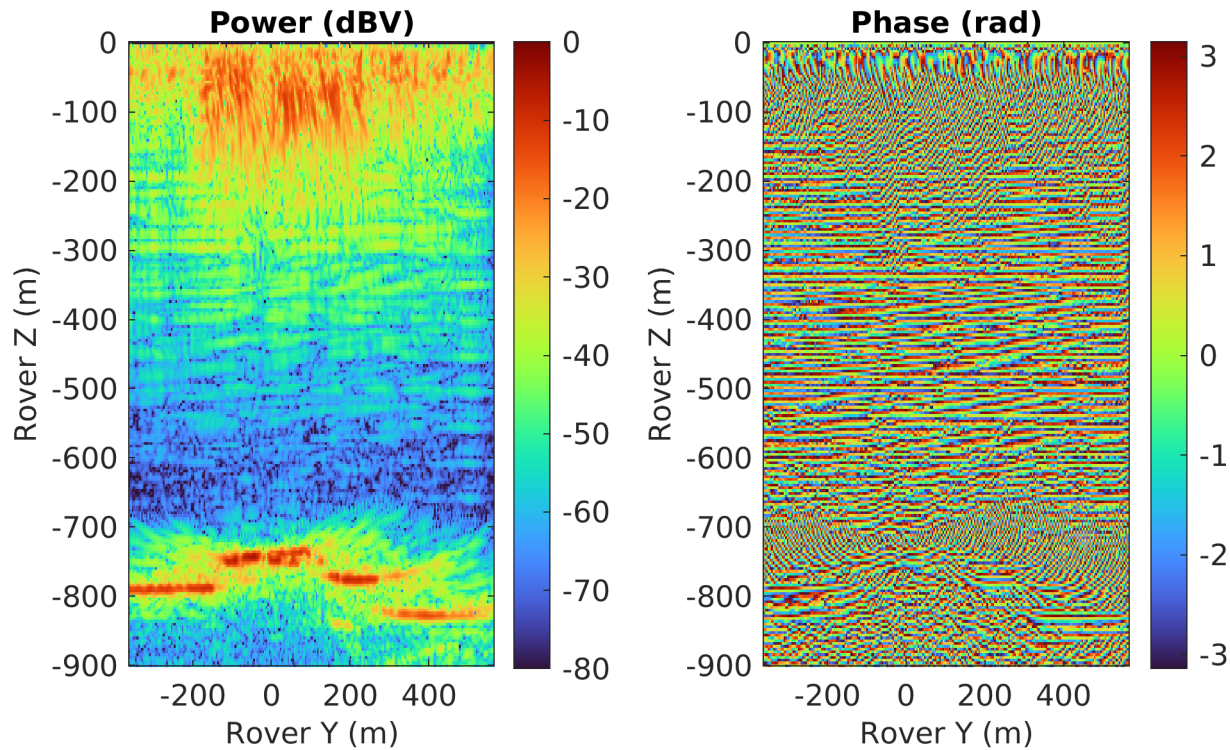


Figure 13: Phase and power of initial backprojected (SAR processed) image from the HF ApRES towed by the SubZero rover. The coordinate system for the image is relative polar stereographic to the Trimble GPS base station. Pixel resolution is 4 m.

### 6.3.2 Kinematic Measurement

The kinematic measurements were made after the start and stop measurements along the same profile to provide a comparative dataset and explore the use of the ApRES radar as a mobile SAR. Processing of the data is underway and not yet included in this report.

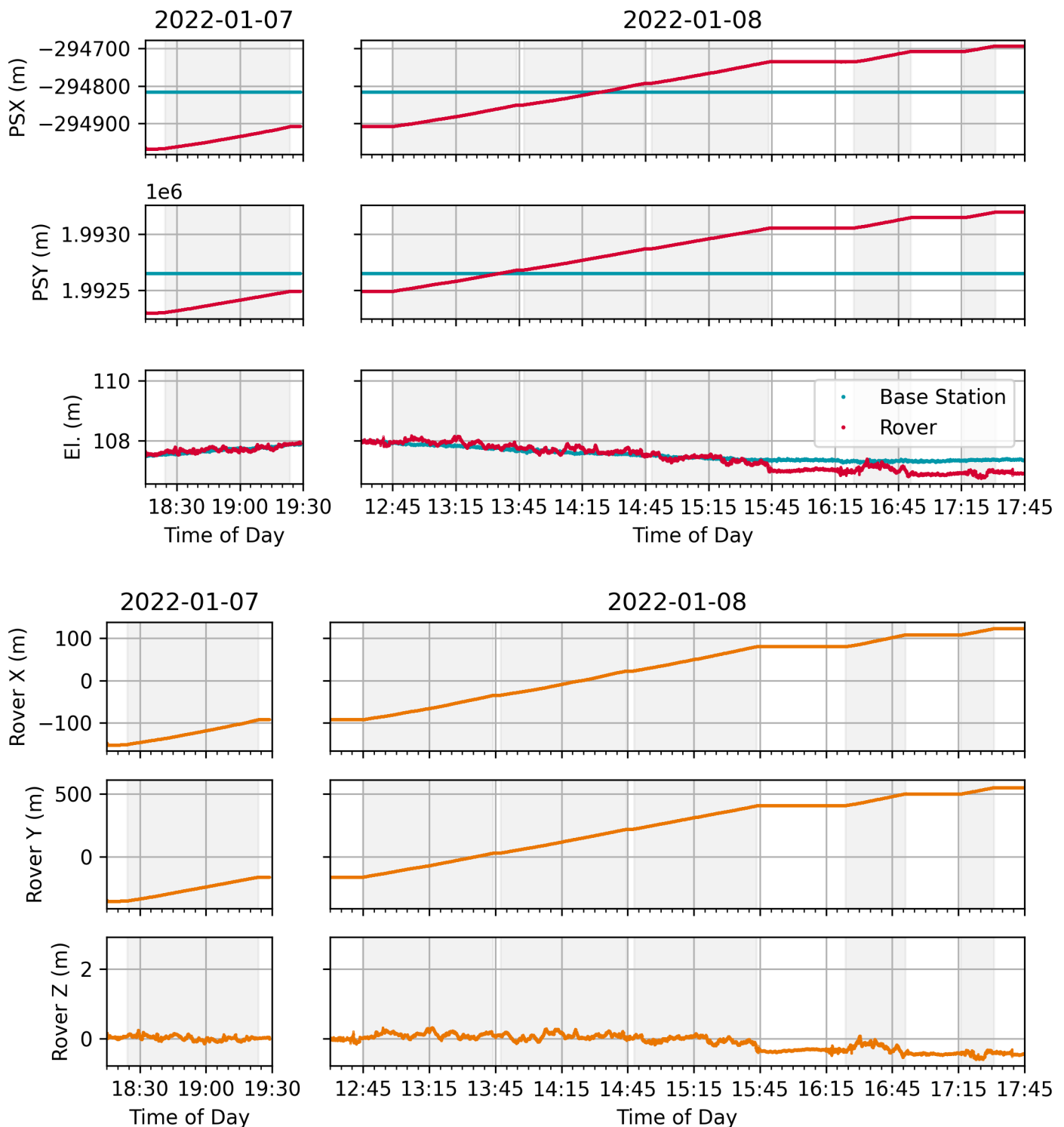


Figure 14: Precise point positioned GPS outputs from Canadian Spatial Reference System for rover and base station. Gray highlighted areas show periods of rover operation. Second plot shows derived relative position of rover to base station, mitigating tidal flexure of ice shelf and positional drift from ice flow.

## 7 cApRES

RE,JH

Name	Date	Latitude	Longitude	pRES	Note
cApRES	10.01.2022	S71 36.9565	W8 25.9803	127	Buried

Table 13: cApRES

The initial cApRES setup used cables of different lengths. One-way travel times for the cables were measured using an SDRKits VNA in time-domain reflectometer (TDR) and network analyser (VNA) modes. The ‘Yellow’ cable was removed from the initial setup and replaced with the ‘Double Earth’ cable to reduce the difference in cable travel time. Final antenna cabling and assignments are listed in Table 14. The ApRES was configured to measure every 3 h, alternating between mono-polarised (HH) and quad-polarised (HH, HV, VH, VV) measurements. The RF attenuator was set to 23 dB and the AF gain was set to  $-14\text{ dB}$ . The chirp settings are the default values with a sweep of 200 MHz to 400 MHz over a period of 1 s.

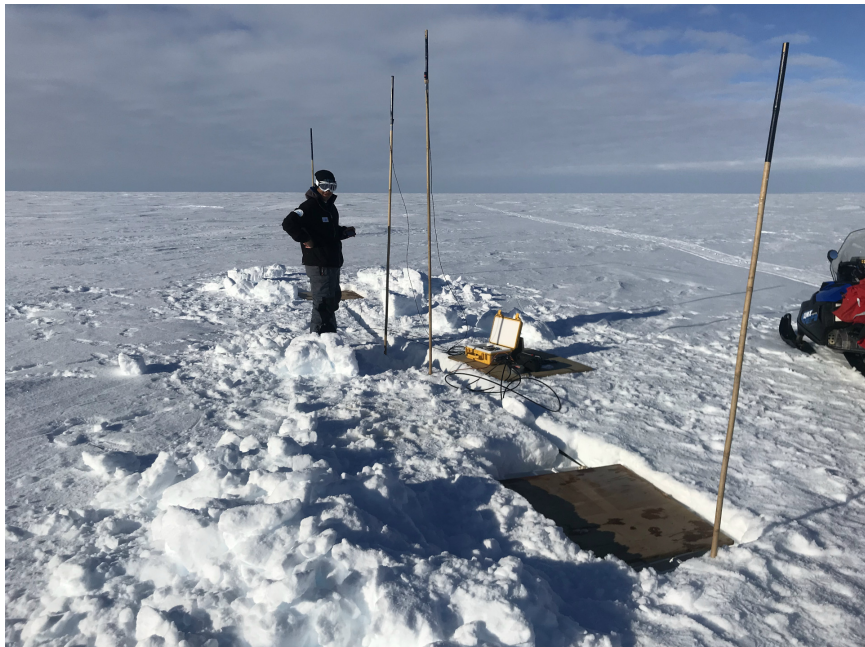


Figure 15: Photograph of cApRES Measurement Setup on 9<sup>th</sup> January 2022, prior to burying of ApRES and replacement of ‘Yellow’ coaxial cable.

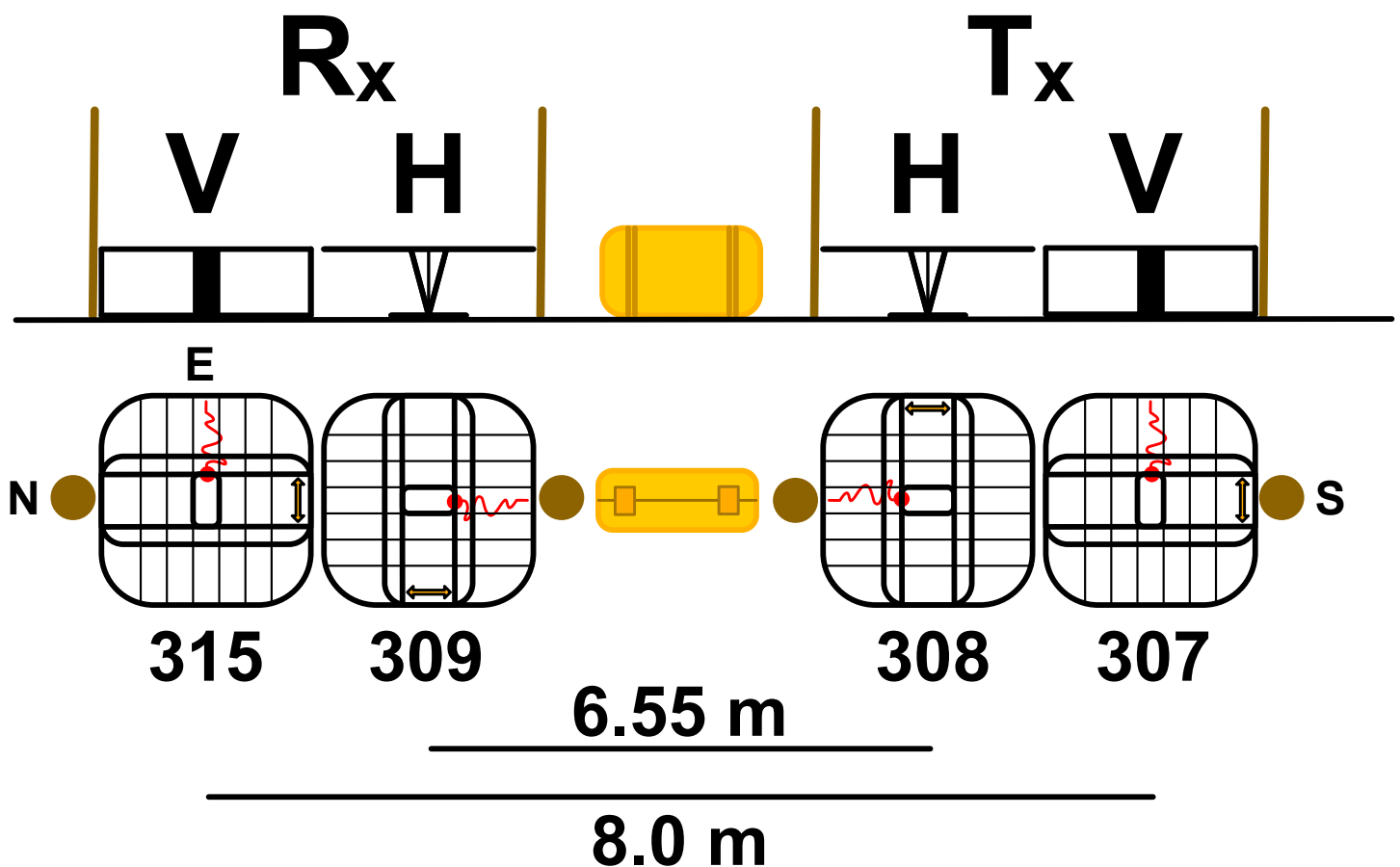


Figure 16: Diagram of cApRES Measurement Setup

Cable Colour	Antenna ID	ApRES Port	Polarisation	1-Way Travel Time (ns)
Blue Earth	315	Rx 2	V	26.69
Double Earth	309	Rx 1	H	26.69
Red	308	Tx 1	H	-
Green	307	Tx 2	V	-
Yellow	Unused	-	-	22.31

Table 14: Antenna and cabling configuration for cApRES measurement setup. One-way travel times for the 'Red' and 'Green' cables were not measured.

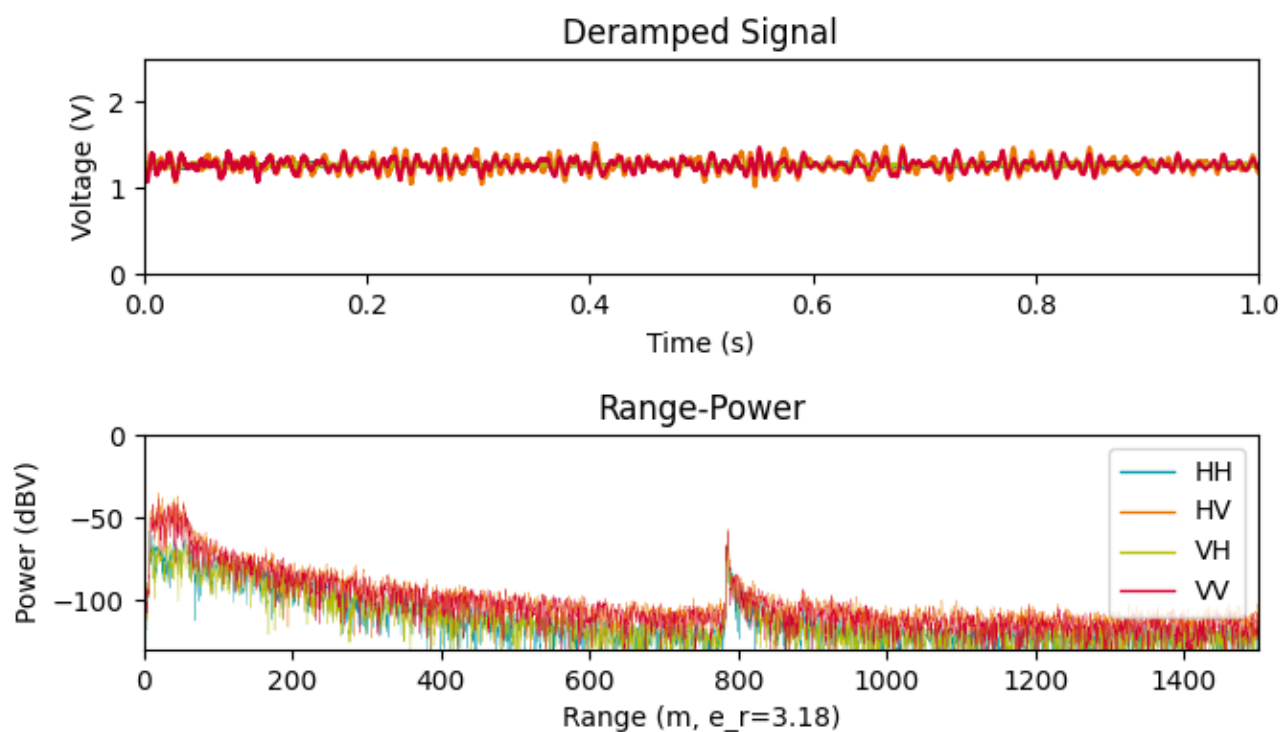


Figure 17: Example data from the cApRES measurement setup taken on 10<sup>th</sup> January 2022 at 18:49:11 UTC.

## 8 Rover-ApRES: Data example, field picture, system setup and site specifics

This section is written by Reza Ershadi ([Email Me](#))

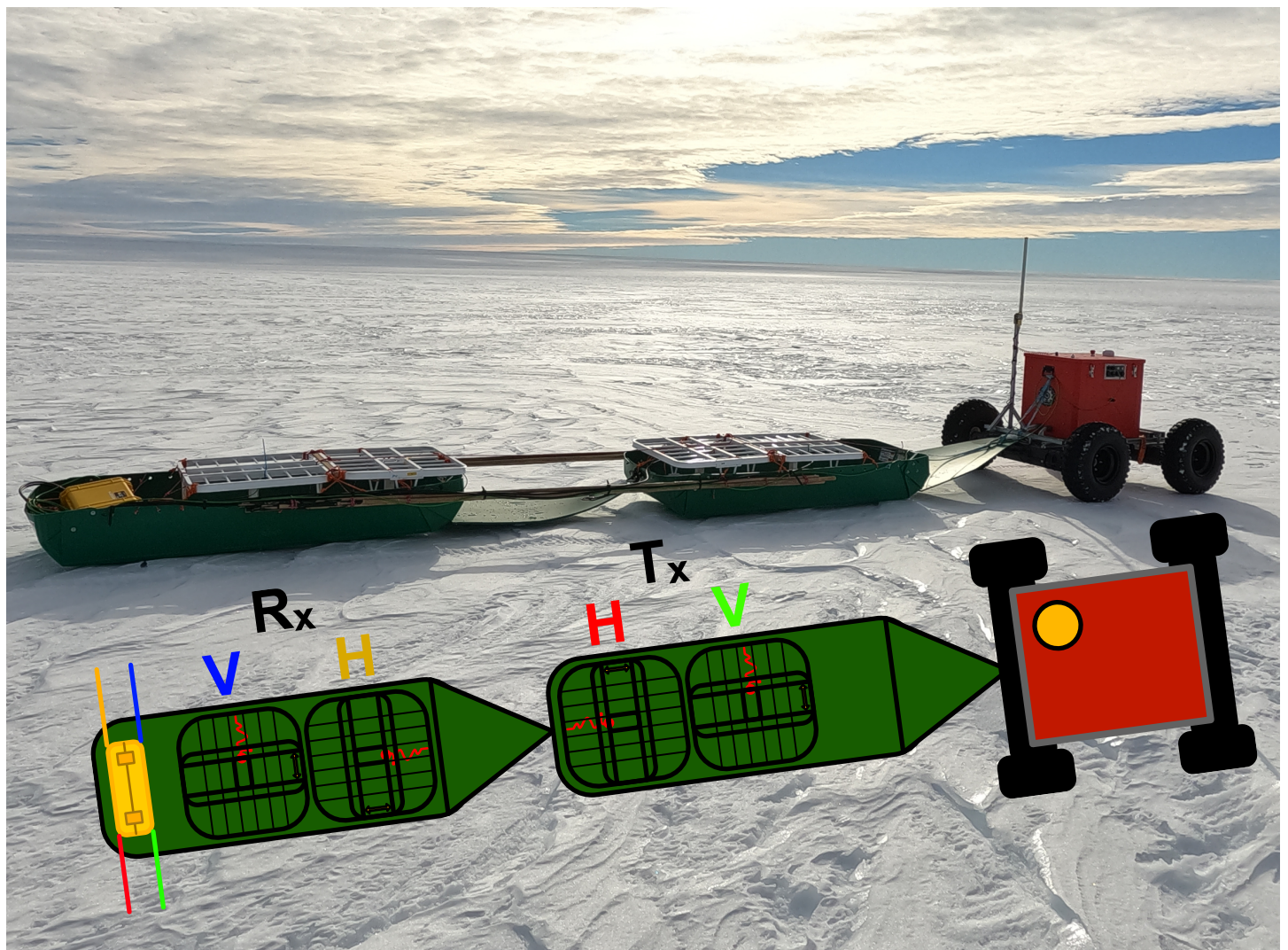


Figure 18: Antenna setup for ApRES profiling with the rover and sleds

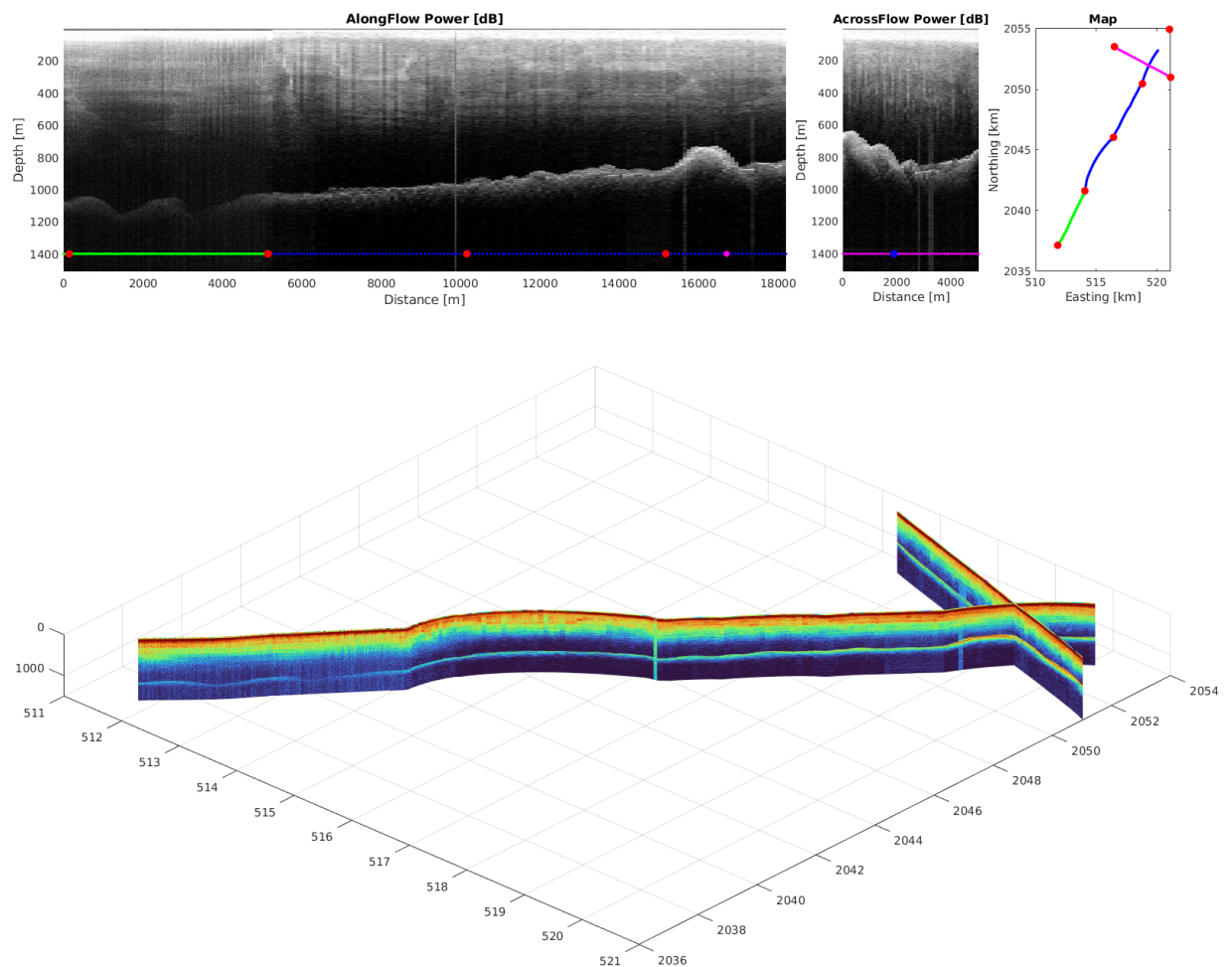


Figure 19: Radar power obtained by the rover-sled profiling system.

## A HF ApRES Database Schemata

### A.1 Table ‘measurements’

Table 15: Specification for `measurements` table.

Fieldname	Datatype	Parameters	Description
measurement_id	INTEGER	PRIMARY KEY	Unique identifier for each file.
filename	TEXT	NOT NULL	Filename without path.
path	TEXT	UNIQUE NOT NULL	Path to file in UNIX form, relative to top-level project root.
name	TEXT	-	The name associated with the measurement, used to group sets of measurements together.
timestamp	TEXT	UNIQUE ASC NOT NULL	YYYY-mm-dd HH:MM:SS.fff formatted timestamp according to time and date the measurement was taken.
valid	INTEGER	NOT NULL DEFAULT 0	Boolean indicator of whether file is valid. Assumes invalid by default.

Table 15: Specification for `measurements` table.

Fieldname	Datatype	Parameters	Description
base_visible	INTEGER	NOT NULL DEFAULT 0	Boolean indicator of whether basal reflector is visible in range data.
base_range_min	REAL	NOT NULL DEFAULT -1	Minimum range (in steps of 50m) at which basal reflector can be found.
base_range_max	REAL	NOT NULL DEFAULT -1	Maximum range (in steps of 50m) at which basal reflector can be found.
location	TEXT	-	Measurement location name.
comments	TEXT	-	Description and comments for measurement if relevant.
latitude	REAL	-	Latitude of measurement location if known.
longitude	REAL	-	Longitude of measurement location if known.
elevation	REAL	-	Elevation of measurement location if known (referenced to WGS84).

Table 15: Specification for `measurements` table.

Fieldname	Datatype	Parameters	Description
tags	TEXT	-	Annotation tags (i.e. <code>bad_chirps</code> , <code>gps_type</code> , ...).

## A.2 Table ‘apres\_metadata’

The fields `id` and `burst_id` make a unique pair to ensure that each burst within a `*.dat` file is only represented once.

Table 16: Specification for `apres_metadata` table.

Fieldname	Datatype	Parameters	Description
<code>id</code>	INTEGER	PRIMARY KEY	Unique identifier for metadata. Distinct from <code>measurement_id</code> in that each <code>*.dat</code> file can have multiple bursts.
<code>burst_id</code>	INTEGER	NOT NULL	Identifies the burst within a <code>*.dat</code> the metadata represents.
<code>measurement_id</code>	INTEGER	NOT NULL	Identifies the file record where the metadata originates from.

### *ApRES Specific Metadata*

<code>timestamp</code>	TEXT	NOT NULL	YYYY-mm-dd HH:MM:SS.ffff formatted timestamp as logged in <code>*.dat</code> file.
<code>n_attenuators</code>	INTEGER	NOT NULL CHECK(>0, <5)	Number of attenuator settings used.
<code>n_chirps</code>	INTEGER	NOT NULL CHECK(>0)	Total number of individual chirps in file.

Table 16: Specification for `apres_metadata` table.

Fieldname	Datatype	Parameters	Description
n_subbursts	INTEGER	NOT NULL CHECK(>0)	Number of sub-bursts (repeats) of the burst configuration.
period	REAL	NOT NULL CHECK(>0)	Chirp period in seconds.
f_lower	REAL	NOT NULL CHECK( $\geq 0$ )	Lower bound of chirp ramp in Hertz.
f_upper	REAL	NOT NULL CHECK( $\geq 0$ )	Upper bound of chirp ramp in Hertz.
af_gain	TEXT	NOT NULL	Comma separated values indicating AF gain settings.
rf_attenuator	TEXT	NOT NULL	Comma separated values indicating RF attenuator settings.
f_sampling	REAL	NOT NULL CHECK(>0)	Sampling frequency.
tx_antenna	TEXT	NOT NULL	Transmit antenna selection in comma separated value format.
rx_antenna	TEXT	NOT NULL	Receive antenna selection in comma separated value format.

Table 16: Specification for `apres_metadata` table.

Fieldname	Datatype	Parameters	Description
power_code	INTEGER	-	DDS output current power code, if available (dependent on firmware).
battery_voltage	REAL	-	Battery voltage, if available.
temperature_1	REAL	-	Measured board temperature from sensor 1.
temperature_2	REAL	-	Measured board temperature from sensor 2.
rmb_issue	TEXT	-	RMB issue number if available.
vab_issue	TEXT	-	VAB issue number if available.
venom_issue	TEXT	-	Venom issue number if available.
software_issue	TEXT	-	VAB firmware issue number if available.